Equivalent Elmore Delay for *RLC* Trees

Yehea I. Ismail, Eby G. Friedman, *Fellow, IEEE*, and José L. Neves

***Abstract*—Closed-form solutions for the 50% delay, rise time, overshoots, and settling time of signals in an RLC tree are presented. These solutions have the same accuracy characteristics of the Elmore delay for RC trees and preserves the simplicity and recursive characteristics of the Elmore delay. Specifically, the complexity of calculating the time domain responses at all the nodes of an RLC tree is linearly proportional to the number of branches in the tree and the solutions are always stable. The closed-form expressions introduced here consider all damping conditions of an RLC circuit including the underdamped response, which is not considered by the Elmore delay due to the nonmonotone nature of the response. The continuous analytical nature of the solutions makes these expressions suitable for design methodologies and optimization techniques. Also, the solutions have significantly improved accuracy as compared to the Elmore delay for an overdamped response. The solutions introduced here for RLC trees can be practically used for the same purposes that the Elmore delay is used for RC trees.**

***Index Terms*—Delay, inductance, interconnect, *RLC*, simulation, tree, VLSI.**

I. Introduction

IT has become well accepted that interconnect delay dominates gate delay in current deep submicrometer very large scale integration (VLSI) circuits [1]–[9]. With the continuous scaling of technology and increased die area, this situation is becoming worse. In order to properly design complex circuits, more accurate interconnect models and signal propagation characterization are required. Initially, interconnect has been modeled as a single lumped capacitance in the analysis of the performance of on-chip interconnects. Currently, RC models are used for high-resistance nets and capacitive models are used for less resistive interconnect [10], [11]. However, inductance is becoming more important with faster on-chip rise times and longer wire lengths. Wide wires are frequently encountered in clock distribution networks and in upper metal layers. These wires are low-resistive wires that can exhibit significant inductive effects. Furthermore, performance requirements are pushing the introduction of new materials for low-resistance interconnect [12]. Inductance is therefore becoming an integral element in VLSI design methodologies, see, e.g., [6], [13], and [14].

Manuscript received December 1, 1998; revised May 4, 1999. This work was supported in part by the National Science Foundation (NSF) under Grant MIP-9610108, the Semiconductor Research Corporation under Contract 99-TJ-687, by a grant from the New York State Science and Technology Foundation to the Center for Advanced Technology-Electronic Imaging Systems, and by grants from the Xerox Corporation, IBM Corporation, Intel Corporation, and Lucent Technologies Corporation. This paper was recommended by Associate Editor E. Bracken.

Y. I. Ismail and E. G. Friedman are with the Department of Electrical and Computer Engineering, University of Rochester, Rochester, NY 14627 USA.

J. L. Neves is with the IBM Microelectronics, East Fishkill, NY 12533 USA.

Publisher Item Identifier S 0278-0070(00)01367-1.

An interconnect line in a VLSI circuit is in general a tree rather than a single line. Thus, the process of characterizing signal waveforms in tree structured interconnect is of primary importance. One of the more popular delay models used within industry for RC trees is the Elmore delay model [15], [16]. Despite not being highly accurate, the Elmore delay is widely used by industry for fast delay estimation. With IC's composed of tens of millions of gates it is often impractical to use highly accurate, time consuming methods to evaluate the delay at each node in the circuit. The Elmore delay model is therefore used to quickly estimate the relative delays of different paths in the circuit, permitting more exhaustive simulations to be performed for only the critical paths. Also, the Elmore delay is widely used as a delay model for the synthesis of VLSI circuits such as buffer insertion in RC trees and wire sizing [17]–[28]. The wide use of the Elmore delay as a basis for design methodologies is primarily because the Elmore delay has a high degree of *fidelity* [17]: an optimal or near-optimal solution achieved by a design methodology based on the Elmore delay is also near-optimal based on a more accurate (e.g., SPICE-computed [24]) delay for routing constructions [25] and wire sizing optimization [23]. Simulations [26] have shown that the clock skew derived under the Elmore delay model has a high correlation with SPICE-derived skew data.

The popularity of the Elmore delay is mainly due to the existence of a simple tractable formula for the delay [29] that has recursive properties [27], making the calculation of the circuit delays highly efficient even in large circuits. No formula for delay calculation has been determined for RLC trees that maintains all the characteristics of the Elmore delay. The absence of an equivalent delay model for RLC trees is primarily due to the fact that the Elmore delay does not cover nonmonotone responses [15] which can occur in RLC circuits. The work described in [30] uses the first and second moments to characterize the response of RLC trees. However, the solutions in [30] are composed of three different formulae for the cases of real, complex, and multiple poles and there are no closed-form solutions for the moments of a tree that can be directly incorporated into the delay model. Furthermore, the solutions in [30] only characterize a step input response and do not characterize the overshoots and settling time of an underdamped response. The focus of this paper is therefore the introduction of a simple tractable delay formula for RLC trees that preserves the useful characteristics of the Elmore delay model while maintaining the same accuracy characteristics. The rise time of the signals in an RLC tree is also characterized as well as the overshoots and the settling time (for an underdamped response).

This paper is organized as follows. A background for calculating the delay in RC and RLC trees is provided in Section II. In Section III, an equivalent second-order approxima-

tion of an RLC tree is developed. Closed-form solutions for the 50% delay, rise time, overshoots, and settling time of the signals within an RLC tree are introduced in Section IV. Accuracy characterization of the proposed delay model is presented in Section V. Finally, some conclusions are offered in Section VI. The algorithmic complexity of the proposed delay model is described in the Appendix.

II. Background

In 1948, Elmore [15] introduced a general approach for calculating the propagation delay of a linear system given its transfer function. If the transfer function of the system is $G(s)$, the normalized transfer function $g(s)$ is $G(s)/G(0)$, which can be generally described as

$$g(s) = \frac{1 + a_1 s + a_2 s^2 + \cdots + a_n s^n}{1 + b_1 s + b^2 s^2 + \cdots + b_m s^m} \tag{1}$$

where a_i and b_i are real and $m > n$. For a monotone response, all the poles of $g(s)$ should be real and for a stable system all the poles should lie on the negative real axis. The unit step response of the normalized transfer function is $(1/s) \cdot g(s)$. In the time domain the transient unit step response $e(t)$ has a final value of one and is monotonically increasing as shown in Fig. 1(a).

Elmore proceeded from the observation that the time domain unit step response has the characteristics of the integral of a probability function since it has a final value of one and is monotonically increasing which makes the area under $e'(t)$ equal to one and makes $e'(t)$ always positive. Thus, Elmore defined the 50% propagation delay [the time where $e(t)$ is equal to 0.5] as

$$T_D = \int_0^\infty te'(t)\,dt \tag{2}$$

which is the centroid of the area under $e'(t)$. By noting that $e'(t)$ for a step input is simply $g(t)$, the transfer function $g(s)$ can be expressed as

$$g(s) = \int_0^\infty e'(t)e^{-st}\,dt = 1 - s\int_0^\infty te'(t)\,dt + \frac{s^2}{2!}\int_0^\infty t^2 e'(t)\,dt - \cdots \tag{3}$$

Thus, if the normalized transfer function is expanded in the powers of s, the 50% delay can be determined directly as the coefficient of s. From (1), the propagation delay is $T_D = b_1 - a_1$ which is the definition of the Elmore delay [15].

In 1987, Wyatt [16] used the relationships that b_1 and a_1 are given by

$$b_1 = \sum_{i=1}^{m} \frac{1}{p_i} \quad \text{and} \quad a_1 = \sum_{i=1}^{n} \frac{1}{z_i} \tag{4}$$

respectively, where p_i and z_i are the poles and zeros of the transfer function, respectively. Thus, Wyatt treated $T_D = b_1 - a_1$ as the reciprocal of the dominant pole (the pole that has the smallest absolute value) of the system. This approximation is accurate for systems that can be modeled by a single dominant pole and has no low-frequency zeros near the dominant pole. Using this approximation, the step response of the system is

$$e(t) = 1 - \exp\left(-\frac{t}{T_D}\right) \tag{5}$$

which indicates a 50% propagation delay equal to $0.693T_D$ rather than T_D as anticipated by Elmore. For example, the simple RC circuit shown in Fig. 2 has the transfer function

$$g(s) = \frac{1}{sRC + 1}. \tag{6}$$

Thus, according to Elmore the propagation delay is RC and according to Wyatt the propagation delay is $0.693RC$. Note that Wyatt's solution is exact for this simple circuit and a step input signal. In general, Wyatt's solution is more accurate than Elmore's solution. Wyatt's approximation is usually still referred to as the Elmore delay.

What has made the Elmore (and Wyatt) delay particularly appealing for RC trees is the introduction of a simple closed-form solution for the time constant T_D [29]. For the RC tree shown in Fig. 3, the time constant T_{Di} at node i is

$$T_{Di} = \sum_k C_k R_{ik} \tag{7}$$

where k is an index that covers each capacitor in the circuit and R_{ik} is the common resistance from the input to the nodes i and

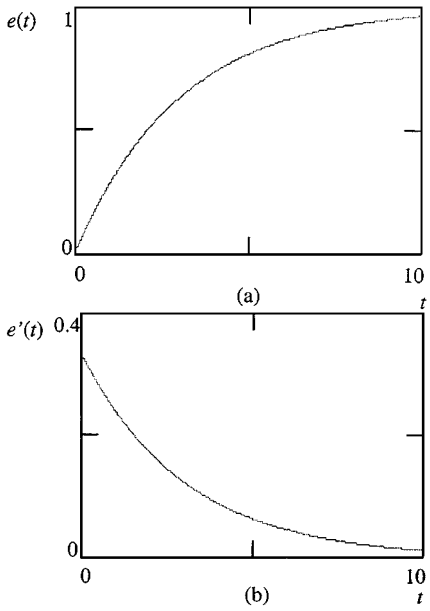

Fig. 1. Step response of a normalized monotone transfer function. (a) Step response. (b) Impulse response (which equals the time derivative of the step response).

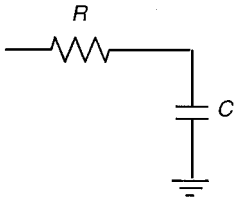

Fig. 2. Simple RC circuit.

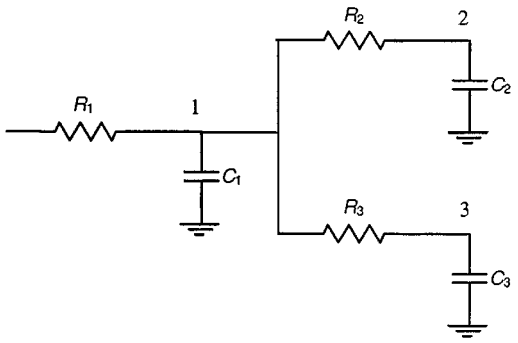

Fig. 3. RLC tree.

k. For example, for the RC tree shown in Fig. 3, $R_{23} = R_1$ and $T_{D2} = C_1 * R_1 + C_2 * (R_1 + R_2) + C_3 * R_1$. Wyatt approximates the transfer function at node i of an RC tree by a first-order (single-pole) transfer function given by

$$g_i(s) = \frac{1}{s \sum_k C_k R_k + 1}. \tag{8}$$

This first-order approximation matches the first moment of the transfer function at node i but approximates the higher-order moments by

$$m_r^i = \left(- \sum_k C_k R_{ik} \right)^r \tag{9}$$

as can be seen in the expansion of (8)

$$\begin{aligned} g_i(s) = & 1 - s \sum_k C_k R_{ik} + s^2 \left(\sum_k C_k R_{ik} \right)^2 \\ & - \cdots = 1 + m_1^i s + m_2^i s^2 + \cdots. \end{aligned} \tag{10}$$

This single pole first-order approximation of the transfer function can be inaccurate in certain cases where arbitrary initial conditions can create a low-frequency zero, thereby violating one of Wyatt's assumptions [31]. For this reason, Horowitz approximates the capacitor voltage with a two pole one zero transfer function by matching boundary conditions [32]. Pillage extended this concept by introducing asymptotic wave evaluation (AWE), which depends on matching the first q moments of the transfer function [33]–[35] rather than only the first moment as Wyatt and Elmore did. This concept allows arbitrary accuracy by including additional moments. The normalized transfer function $g(s)$ can be expanded in the powers of s as

$$g(s) = 1 + m_1 s + m_2 s^2 + \cdots \tag{11}$$

where m_i is the ith moment of the transfer function [33]. The first $2q$ moments of the transfer function include the information needed to calculate the first q poles and the residues of these poles. Numerical methods have been developed [34]–[37] to efficiently calculate the moments, poles, and residues. Also, model-order reduction techniques based on the state-space representation of an RLC network have been used to calculate the transient response of signals within the tree such as: pade via lanczos (PVL) [38], matrix pade via lanczos (MPVL) [39], arnoldi algorithm [40], block arnoldi algorithm [41], passive reduced-order interconnect macromodeling algorithm (PRIMA) [42], [43], and SyPVL Algorithm [44]. However, the Elmore (Wyatt) delay is still widely used within industry since it is computationally faster to evaluate and always leads to stable solutions. Also, due to the existence of a closed-form tractable solution, the Elmore delay is amenable to synthesis and VLSI-oriented design methodologies. Asymptotic wave evaluation is mainly used in analyzing those networks that require high accuracy and covers both monotone and nonmonotone responses. In [45], the first and second moments are used to evaluate the delay of a VLSI interconnect. However, no closed-form solution is described for RLC trees.

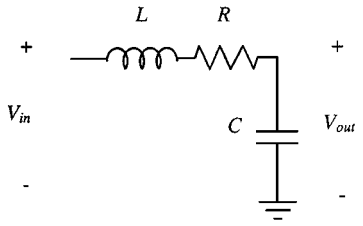

Fig. 4. Simple RLC circuit.

III. Second-Order Approximation for RLC Trees

As mentioned previously, the Elmore (Wyatt) delay does not properly characterize RLC networks due to the possibility of a nonmonotone response of an RLC network. To illustrate this point, consider the simple single -section RLC circuit depicted in Fig. 4. This circuit has a second-order transfer function that can be characterized by

$$g(s) = \frac{1}{s^2 LC + sRC + 1}. \tag{12}$$

Note that the coefficient of s^1 is RC, which does not include the inductance L. This coefficient of the Elmore time constant (and thus the Wyatt approximation) does not depend on the inductance. However, inductance can have a significant effect on the response of the circuit. To better observe the effects of inductance, the transfer function of the circuit can be reconfigured as

$$g(s) = \frac{\omega_n^2}{s^2 + s 2\zeta\omega_n + \omega_n^2} \tag{13}$$

where

$$\zeta = \frac{1}{2} \frac{RC}{\sqrt{LC}} \tag{14}$$

$$\omega_n = \frac{1}{\sqrt{LC}}. \tag{15}$$

The poles of the transfer function are

$$P_{1,2} = \omega_n \left[-\zeta \pm \sqrt{\zeta^2 - 1} \right]. \tag{16}$$

Note that if ζ is less than one, the poles are complex and oscillations occur in the response which violates the monotone re-

sponse condition of the Elmore delay. In this case, the response is underdamped and overshoots occur. If ζ is greater than one, the poles are real and the response is an overdamped response. If ζ is equal to one, the response is a critically damped response. ζ is called the damping factor of the system. From (14), as the inductance increases, ζ decreases which violates the assumption of a monotonic response.

At least a second-order approximation is required to characterize a nonmonotone response, because a nonmonotone response involves complex poles which appear in conjugate pairs in a real system. Thus, a second-order system such as (13) can be used to approximate a system with a nonmonotone response. It is therefore necessary to determine ζ and ω_n in order to make the second-order approximation as accurate as possible as compared to the exact transfer function. The transfer function in (13) can be expanded in powers of s where the first two moments of the transfer function are equated to the first two moments of the system, m_1 and m_2. The expansion of the transfer function in (13) is

$$g(s) = 1 - s\left(\frac{2\zeta}{\omega_n}\right) + s^2\left(\frac{-1+(2\zeta)^2}{\omega_n^2}\right) - \cdots = 1 + m_1 s + m_2 s^2 + \cdots. \tag{17}$$

The parameters that characterize the second-order approximation of a nonmonotonic system, ζ and ω_n, can be calculated in terms of the moments of the nonmonotonic system and are

$$\zeta = \frac{-m_1}{2}\ \frac{1}{\sqrt{m_1^2 - m_2}} \tag{18}$$

$$\omega_n = \frac{1}{\sqrt{m_1^2 - m_2}}. \tag{19}$$

Hence, for a system with a nonmonotonic response a second-order approximation can be found if the first and second moments of the system are known.

For the general RLC tree shown in Fig. 5, the voltage drop at any node i as compared to the input voltage is

$$V_{in}(s) - V_i(s) = \sum_k C_k V_k(s) s[R_{ki} + L_{ki} s]. \tag{20}$$

If the input is a unit impulse, $V_{in}(s)$ is equal to 1.0 and the voltages at the nodes of the tree are the unit impulse responses of these nodes. Thus, the normalized transfer function $g_i(s)$ at node i is given by $V_i(s)$ and is

$$g_i(s) = 1 - \sum_k C_k V_k(s) s[R_{ki} + L_{ki} s] = 1 + m_1^i s + m_2^i s^2 + \cdots. \tag{21}$$

The first and second moments at node i can be derived from

$$m_1^i = \left.\frac{dg_i(s)}{ds}\right|_{i=0} \tag{22}$$

$$m_2^i = \frac{1}{2!}\ \left.\frac{d^2 g_i(s)}{ds^2}\right|_{s=0}. \tag{23}$$

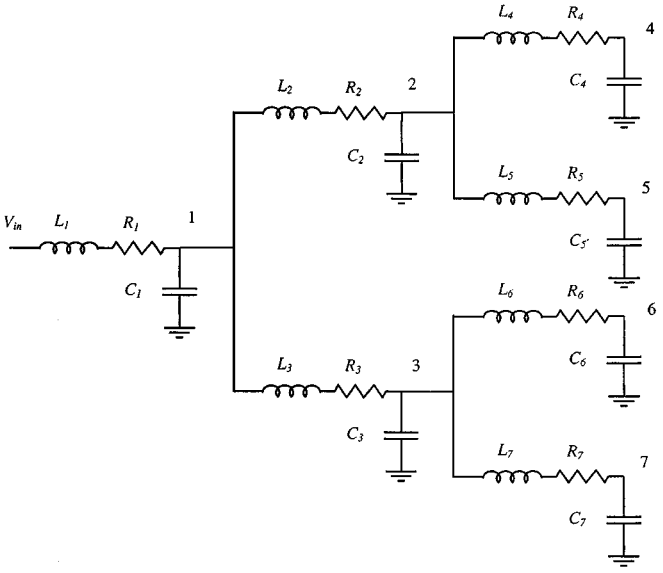

Fig. 5. General RLC tree.

Differentiating (21) with respect to s and substituting $s = 0$

$$m_1^i = -\sum_k C_k R_{ik} V_k(s)|_{s=0} \tag{24}$$

$$m_2^i = -\sum_k C_k R_{ik}\ \left.\frac{dV_k(s)}{ds}\right|_{s=0} - \sum_k C_k L_{ik} V_k(s)|_{s=0}. \tag{25}$$

Note that $V_k(s)|_{s=0} = 1$ and $dV_k(s)/ds|_{s=0} = m_1^k$ since $V_k(s0 = g_k(s) = 1 + m_1^k s + m_2^k s^2 + \cdots$. Thus, the first and second moments of a general RLC tree at node i are

$$m_1^i = -\sum_k C_k R_{ik} \tag{26}$$

$$m_2^i = \sum_k \sum_j C_k R_{ik} C_j R_{kj} - \sum_k C_k L_{ik}. \tag{27}$$

Since the Elmore (Wyatt) model approximates the first term in m_2^i by $(\Sigma_k\ C_k R_{ik})^2$, a similar approximation is used here. Thus, the second moment is approximated by

$$m_2^i = \left(\sum_k C_k R_{ik}\right)^2 - \sum_k C_k L_{ik}. \tag{28}$$

Substituting the first and second moments of a general RLC tree into (18), ζ_i and ω_{ni} that characterize a second-order approximation of the transfer function at node i are

$$\zeta_i = \frac{1}{2}\ \frac{\sum_k C_k R_{ik}}{\sqrt{\sum_k C_k L_{ik}}} \tag{29}$$

$$\omega_{ni} = \frac{1}{\sqrt{\sum_k C_k L_{ik}}}. \tag{30}$$

Note the analogy with ζ and ω_n for a single RLC section in (14) and (15). The time constants RC and $\sqrt{LC}$ are replaced by the summations of the equivalent time constants in the tree. Note also that (29) and (30) becomes (14) and (15), respectively, for a single section. This second-order approximation has the same accuracy characteristics as that of the Elmore (Wyatt) approximation for an RC tree. The accuracy characteristics of this second-order approximation is discussed in Section V.

IV. Signal Characterization in RLC Trees for a Step Input

The second-order approximation of the transfer function of an RLC tree at node i described by (13), (29) and (30) can be used to determine the time domain signal at node i for an arbitrary input. The Laplace transform of the input is multiplied by the second-order approximate transfer function. The inverse Laplace transform is calculated for the resulting expression to determine the time domain signal. After determining an expression that describes the time domain signal at node i of an RLC tree, an iterative method is applied to calculate the primary parameters that characterize the time domain response such as the 50% propagation delay and the 90% rise time. However, for the special case of a step input, these parameters can be calculated directly without applying the aforementioned procedure due to the mathematical nature of the time domain signal.

For a step input and a supply voltage of V_{DD}, the time domain response at node i derived from the second-order approximation is

$$S_i(t) = V_{DD} + \frac{V_{DD}}{2\sqrt{\zeta_i^2-1}}\left[\frac{\exp\left[\omega_{ni}t\left(-\zeta_i+\sqrt{\zeta_i^2-1}\right)\right]}{-\zeta_i+\sqrt{\zeta_i^2-1}} - \frac{\exp\left[\omega_{ni}t\left(-\zeta_i-\sqrt{\zeta_i^2-1}\right)\right]}{-\zeta_i-\sqrt{\zeta_i^2-1}}\right]. \tag{31}$$

The rise time is defined here as the time for the signal to rise from 10% to 90% of the final value. Also, the overshoots and the settling time for the case of an underdamped response are characterized. In the step response in (31), note that time is always multiplied by ω_{ni}. Thus, if the time is scaled by ω_{ni}, the step response at node i with a supply voltage of V_{DD} volts becomes a function of only one variable ζ_i and is

$$S_i'(t) = V_{DD} + \frac{V_{DD}}{2\sqrt{\zeta_i^2-1}}\left[\frac{\exp\left[t'\left(-\zeta_i+\sqrt{\zeta_i^2-1}\right)\right]}{-\zeta_i+\sqrt{\zeta_i^2-1}} - \frac{\exp\left[t'\left(-\zeta_i-\sqrt{\zeta_i^2-1}\right)\right]}{-\zeta_i-\sqrt{\zeta_i^2-1}}\right] \tag{32}$$

where $S_i'(t)$ is the time scaled response at node i and t' is time scaled by ω_{ni}. The time scaled 50% delay and rise time can be calculated by equating $S_i'(t)$ to $0.5V_{DD}$, $0.1V_{DD}$, and $0.9V_{DD}$, respectively. The time scaled 50% delay at node i and the rise time are only functions of one variable ζ_i. The 50% delay and the rise time calculated for several values of ζ_i are plotted as functions of ζ_i in Fig. 6. A curve fitting method is applied to characterize the time scaled 50% delay and rise time as functions of ζ_i and these functions are

$$t'_{pdi} = 1.047e^{(\zeta_i/0.85)} + 1.39\zeta_i \tag{33}$$

$$t'_{ri} = 6.017e^{\left(\zeta_i^{1.35}/0.4\right)} - re^{\left(\zeta_i^{1.25}/0.64\right)} + 4.39\zeta_i \tag{34}$$

where t'_{pdi} and t'_{ri} are the time scaled 50% delay and rise time at node i, respectively. The 50% delay and rise time at node i can be determined by dividing t'_{pdi} and t'_{ri} by ω_{ni} and are

$$t_{pdi} = \left(1.047e^{(\zeta_i/0.85)} + 1.39\zeta_i\right)/\omega_{ni} \tag{35}$$

$$t_{ri} = \left(6.017e^{\left(\zeta_i^{1.35}/0.4\right)} - 5e^{\left(\zeta_i^{1.25}/0.64\right)} + 4.39\zeta_i\right)/\omega_{ni}. \tag{36}$$

Note that the 50% delay and the rise time at node i can be described as

$$t_{pdi} = \left(1.047e^{(\zeta_i/0.85)}\right)/\omega_{ni} + 0.695\sum_k C_k R_{ik} \tag{37}$$

$$t_{ri} = \left(6.017e^{\left(\zeta_i^{1.35}/0.4\right)} - 5e^{\left(\zeta_i^{1.25}/0.64\right)}\right)/\omega_{ni} + 2.195\sum_k C_k R_{ik}. \tag{38}$$

For large ζ_i (low inductance effects), these solutions become the Elmore (Wyatt) approximation of the 50% delay and the rise time for an RC tree at node i. This relationship between (37) and (38) for large ζ_i and the Elmore (Wyatt) delay demonstrates that the general solutions for the 50% delay and the rise time introduced here include the Elmore (Wyatt) delay for the special case of an RC tree. Note also that the general solutions introduced here include all types of responses (underdamped nonmonotone, critically damped, and overdamped) in one continuous equation, which is useful in applications such as buffer insertion, wire sizing, and other VLSI-based design, synthesis, and analysis methodologies.

For the case of an underdamped nonmonotone response when $\zeta_i < 1$ (see Fig. 7), overshoots and undershoots occur which must also be characterized. Also, another parameter can be used to characterize nonmonotone responses and is defined as the time when the oscillations about the steady state are smaller than x of the steady state value. This parameter is usually called the settling time and x is typically chosen to be 0.1 [47]. The value of the maximum or minimum oscillations can be found by differentiating (31) with respect to time and equating the result

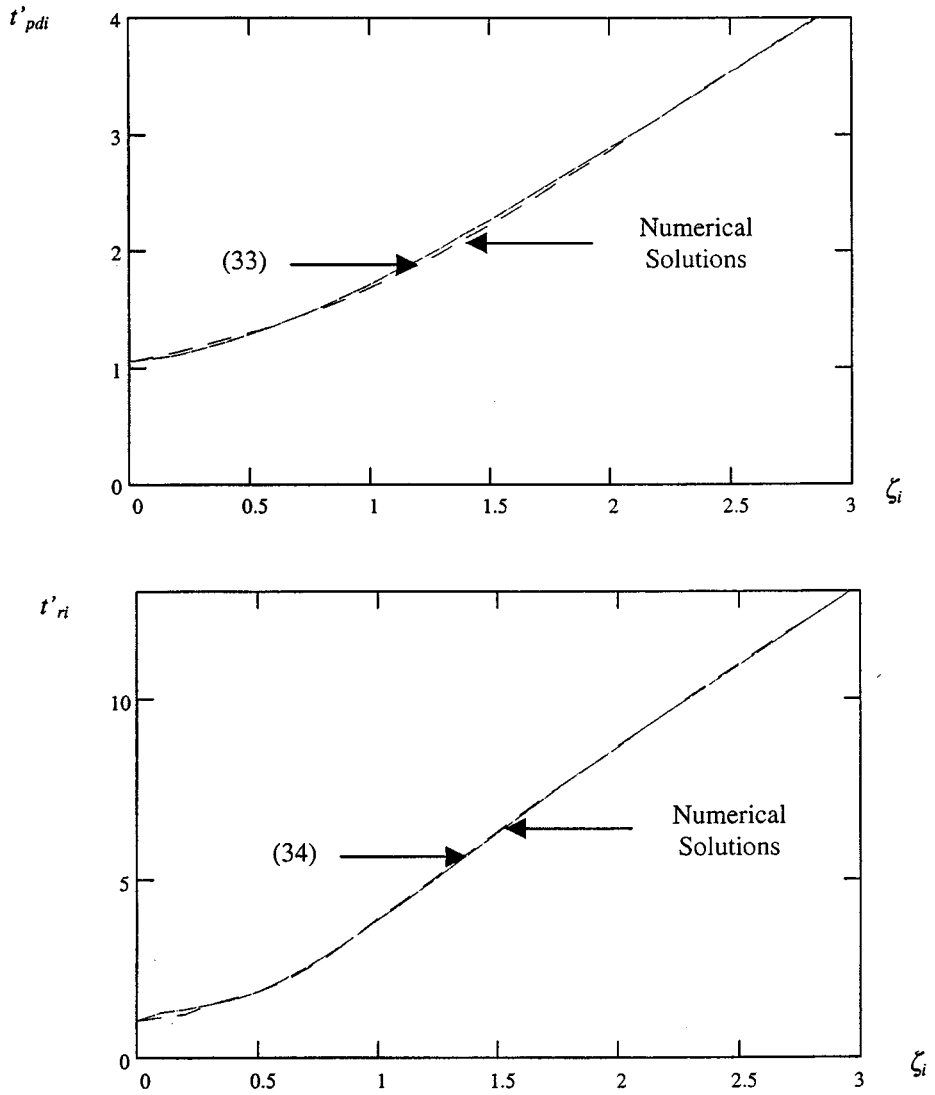

Fig. 6. The time scaled 50% delay and rise time, t'_{pdi} and t'_{ri}, versus ζ_i. (33) and (34) are also shown.

to zero. The values for the maximum or minimum oscillations at node i as a percentage of the final value are given by

$$\%O_i = (-1)^{n+1} \cdot 100 \exp\left(-\frac{n\pi\zeta_i}{\sqrt{1-\zeta_i^2}}\right) \qquad n = 1, 2, \cdots \tag{39}$$

where $\%O_i$ represents the maximum overshoots for n odd and minimum undershoots for n even at node i. The time at which the nth overshoot occurs at node i is

$$t_{Oi} = \frac{n\pi}{\omega_{ni}\sqrt{1-\zeta_i^2}}. \tag{40}$$

The settling time can be calculated by equating $\%O_i$ to $x*100$ to determine n which represents the first overshoot that is less than x times the steady state value. The time of this overshoot is the settling time and can be calculated by substituting n calculated from $\%O_i = x*100$ in (41). Thus, the settling time at node i is

$$t_{si} = \frac{-\ln(x)}{\zeta_i\omega_{ni}}. \tag{41}$$

For $x = 0.1, t_{si}$ is

$$t_{si} = \frac{2.3}{\zeta_i\omega_{ni}}. \tag{42}$$

V. Accuracy Characterization of the Second-Order Approximation

The accuracy characteristics of the second-order approximation introduced in Section III are discussed and explained in this section. The effect of the signal applied at the input of the tree on the accuracy of the second-order approximation is discussed in Section V-A. The effects of the unbalance in impedances within the tree and the branching factor for balanced trees are discussed in Sections V-B and V-C, respectively. The effect of the depth of the tree is discussed in Section V-D. The effect of the position with respect to the source of the node at which the response is evaluated is presented in Section V-E. Finally, the effect of higher-order oscillations in the response is discussed in Section V-F. In general, the approximation introduced here for RLC trees has the same accuracy characteristics as that of the Elmore

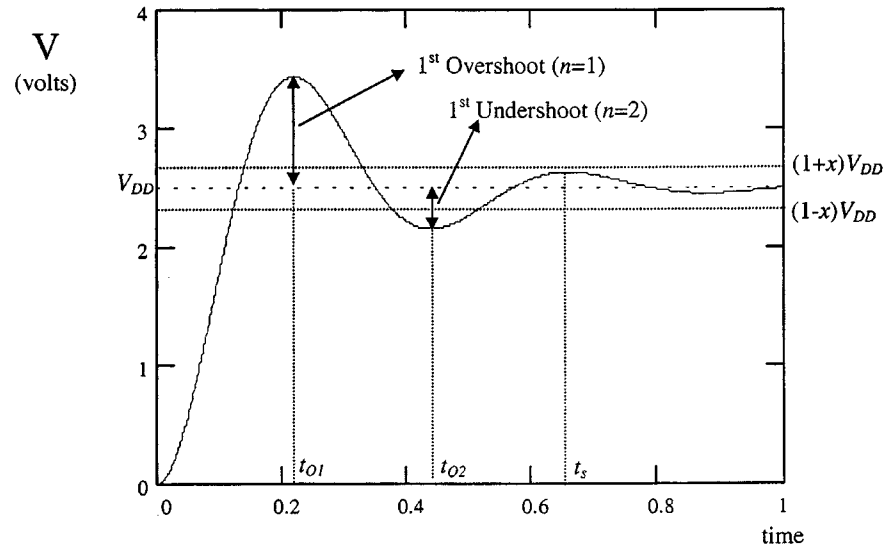

Fig. 7. Characterization of an underdamped response. V_{DD} is the supply voltage. x is the ratio of the final value which bounds the oscillations for the response to be considered settled. The times $t_{O1}, t_{O2}, \cdots$ are the times at which the overshoots and undershoots occur. t_s is the settling time.

(Wyatt) delay for RC trees. Expression (35) in Section IV is used to calculate the propagation delay throughout this section.

A. Effect of the Input Waveform Shape

As mentioned in Section IV, the second-order approximation introduced in this paper in (13), (29) and (30) can be used to calculate the time domain response of an arbitrary input signal. The error of the time domain response calculated using the second-order approximation as compared to AS/X [46] simulations is dependent on the characteristic of the input signal. More specifically, the calculated time domain response becomes more accurate as the rise time of the input signal increases. To illustrate this behavior, an exponential input signal of the form

$$V_{in}(t) = V_{DD}[1 - \exp(-t/\tau)]u(t) \tag{43}$$

is applied to the second-order approximation where $u(t)$ is the unit step function, V_{DD} is the supply voltage, and the 90% rise time of the input signal is 2.3τ. τ is the time constant of the exponential in (27). Note that an exponential signal more accurately characterizes the signals in VLSI circuits as compared to a ramp input signal. The time domain response at node i of an RLC tree for this exponential input is

$$e_{i_{RLC}}(t) = V_{DD}\left[1 - ke^{-(t/\tau)} + \frac{e^{-\zeta_i\omega_{ni}t}}{\sqrt{1-\zeta_i^2}} \cdot \left[\sin(\omega_{ni}t - \theta_1) - \sqrt{\frac{1}{k}}\sin(\omega_{ni}t - \theta_2)\right]\right] \tag{44}$$

where

$$\theta_1 = \tan^{-1}\left[\frac{\sqrt{1-\zeta_i^2}}{\zeta_i}\right] \tag{45}$$

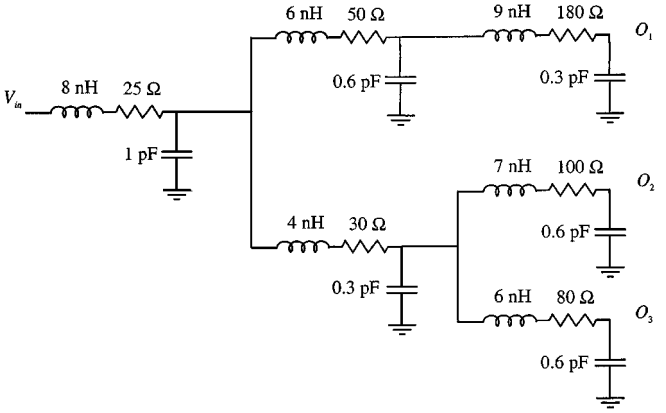

Fig. 8. An example of an RLC tree.

$$\theta_2 = \tan^{-1}\left[\frac{\left(\frac{\tau}{T_{LCi}}\right)\sqrt{1-\zeta_i^2}}{\left(\frac{\tau}{T_{LCi}}\right)\zeta_i - 1}\right] \tag{46}$$

and

$$k = \frac{\left(\frac{\tau}{T_{LCi}}\right)^2}{\left(\frac{\tau}{T_{LCi}}\right)^2 - 2\zeta\left(\frac{\tau}{T_{LCi}}\right) + 1}. \tag{47}$$

T_{LCi} is

$$T_{LCi} = \sqrt{\sum_k C_k L_{ik}}. \tag{48}$$

This closed-form time domain solution is evaluated for output O_2 of the RLC tree shown in Fig. 8 and is compared to AS/X [46] simulations in Fig. 9. Note in Fig. 9 that as the rise time of the input signal increases as compared to T_{LCi}, the calculated time domain response becomes more accurate. This relationship

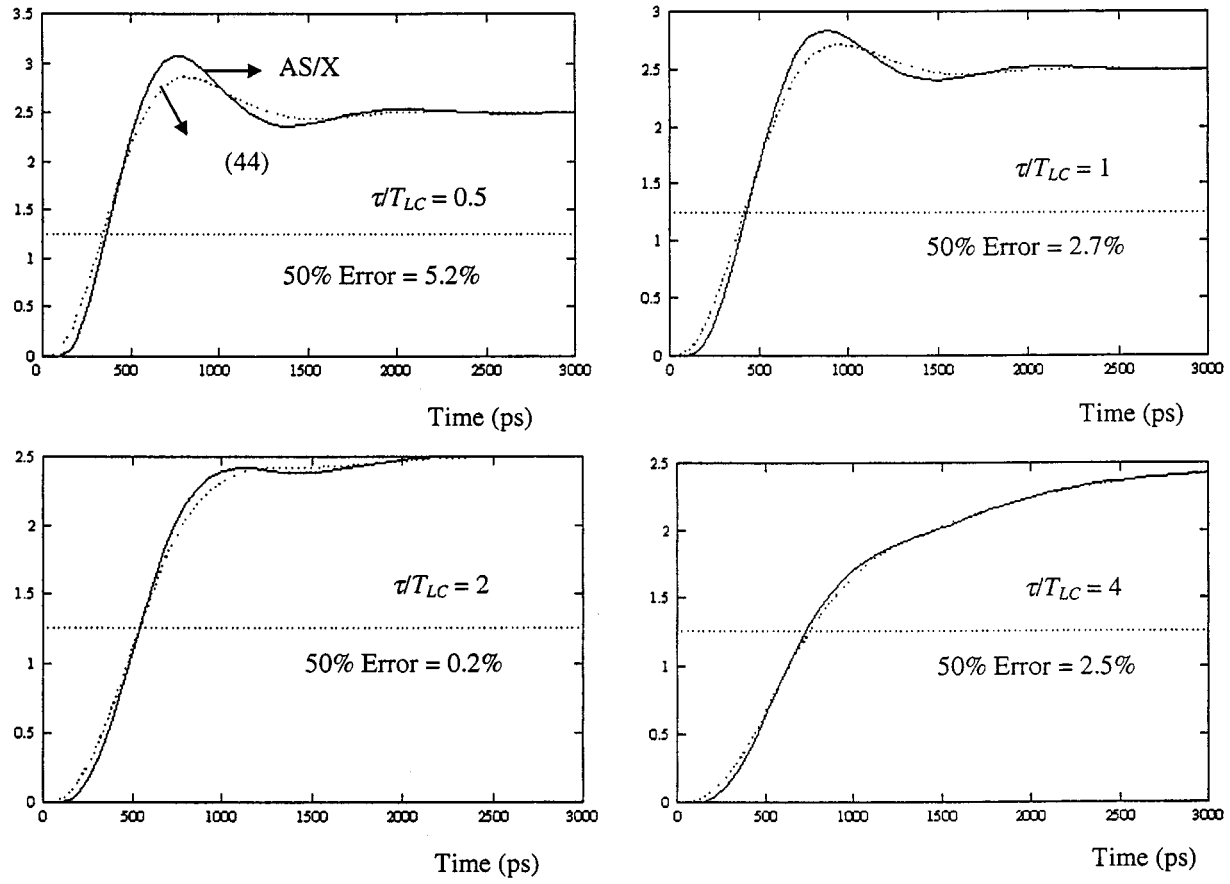

Fig. 9. Simulations of the time domain response for output O_2 of the tree shown in Fig. 8 as compared to the closed-form solution in (43) for different input rise times.

is intuitive since the closed-form solution accurately captures the characteristics of the input signal. As the input rise time increases as compared to the time constants of the impedances within the RLC tree, the dependence of the output response on the input signal increases as compared to the dependence on the characteristics of the RLC tree. Hence, the output response becomes more accurate when the response is dominated by the input characteristics, which are accurately captured by the closed-form solution. Thus, an argument can be made that the time domain response calculated using the second-order approximation introduced here is largest for a step input (which has a zero rise time).

B. Effect of Unbalanced Impedances within the RLC Tree

A balanced tree is a tree where the impedances of the RLC sections that constitute each level are equal, making the paths to all the sinks identical. For example, the tree shown in Fig. 5 is balanced if the RLC sections, 2 and 3, which constitute the second level of the tree are identical and the RLC sections, 4, 5, 6, and 7, which constitute the third level are identical. If the tree in Fig. 5 is not balanced, the transfer function at any of the sinks (nodes 4, 5, 6, or 7) is of order 14 since the tree has seven capacitors and seven inductors. The transfer function at any of the sinks has six of the 14 zeros (the total number of zeros is always equal to the total number of poles) at infinity since there are three shunt capacitors and three series inductors from the input to each sink. The remaining eight zeros are finite zeros

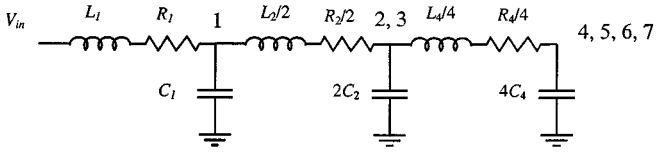

Fig. 10. Equivalent ladder circuit of the RLC tree shown in Fig. 5 when the tree is balanced.

making the order of the numerator eight. When the tree is balanced, an exact calculation of the transfer function illustrates that the eight finite zeros of the transfer function coincide with eight of the poles. These eight poles and zeros cancel, leaving the transfer function at the sinks only of order six with no finite zeros. To better interpret this behavior, note that nodes 2 and 3 can be shunted when the tree shown in Fig. 5 is balanced due to symmetry without affecting the response at any node of the tree. Also, nodes 4, 5, 6, and 7 can be shunted due to symmetry. Thus, the RLC tree shown in Fig. 5 is equivalent to the ladder circuit shown in Fig. 10 after calculating the equivalent impedance of the parallel RLC sections. This ladder circuit has a transfer function of order six at the output with no finite zeros. Note that if the tree has a fourth level, the eight RLC sections of that level correspond to one RLC section in the equivalent ladder circuit. In the fifth level, 16 RLC sections correspond to one RLC section in the equivalent ladder circuit. Thus, the number of poles of the transfer function at the sinks of a balanced RLC tree increases linearly with the number of levels in

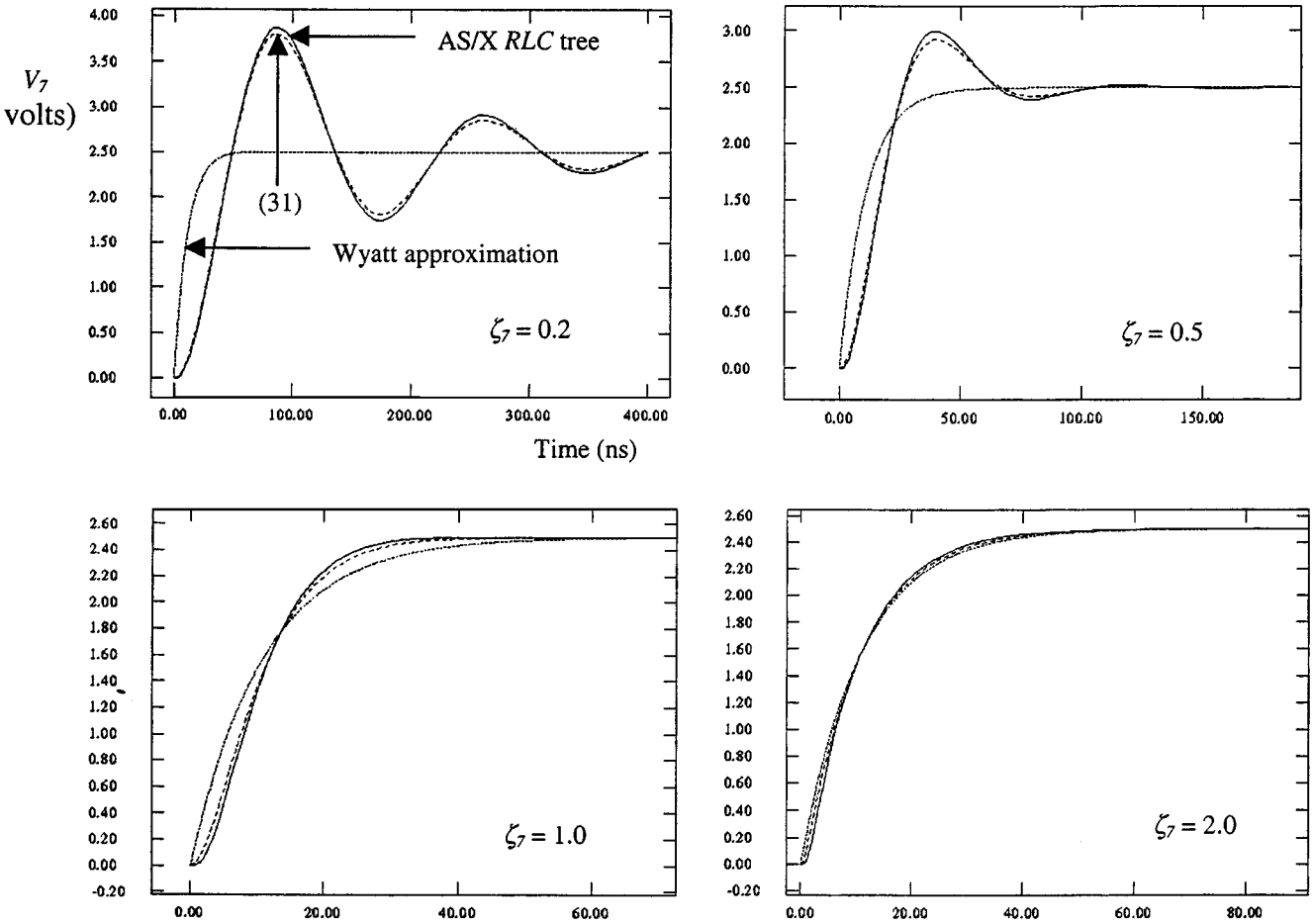

Fig. 11. AS/X simulations as compared to (31) for several values of ζ. The Elmore (Wyatt) solution is also shown. Results are for node 7 for the circuit shown in Fig. 5.

the tree due to pole-zero cancellation. Note that no finite zeros are added by increasing the number of levels. For an unbalanced RLC tree with a binary branching factor, the number of poles and finite zeros at the sinks increases exponentially with the number of levels in the tree. The second-order approximation used here has two poles and no finite zeros and more accurately approximates the transfer function of a balanced RLC tree than that of an unbalanced tree.

The closed-form solution is compared to AS/X [46] simulations of the tree shown in Fig. 5 at output node 7. The simulations are shown in Fig. 11 for a balanced tree with several values of ζ_7 (the equivalent damping factor at node 7) and a step input which represents the highest error as discussed in subsection A. The Elmore (Wyatt) solution is also shown for comparison. Note the high accuracy that the solution exhibits as compared to the AS/X simulations for the case of a balanced tree. The error in the propagation delay is less than 4% for this balanced tree example. The accuracy of the solution introduced here deteriorates as the tree becomes more asymmetric. To quantify the error between the closed-form solution introduced here and AS/X simulations, simulations and analytic solutions of several asymmetric trees are shown in Fig. 12 The parameter *asym* is introduced to quantify the relative asymmetry of an RLC tree. For example, when *asym* is equal to two, the impedance of the left branch is always twice the impedance of the right branch. The higher *asym*, the greater the asymmetry of the tree. The error in the propagation delay can reach 20% for highly asymmetric trees. The error in the waveform shape is even higher as compared to AS/X simulations. These characteristics, however, are also typical for the Elmore (Wyatt) approximation for RC trees.

C. Effect of the Branching Factor for Balanced Trees

An RLC tree with a binary branching factor and n levels has $2^n - 1$ branches. As shown in Section V-B, the tree is equivalent to a ladder circuit with n RLC sections if the tree is balanced due to pole-zero cancellation. The second-order approximation is more accurate for balanced trees because of this exponential pole-zero cancellation. A tree with a general branching factor B and n levels has $(B^n - 1)/(B - 1)$ branches. However, if the tree is balanced, the tree is again equivalent to a ladder circuit with n RLC sections. Thus, a higher number of zeros are canceled by poles by increasing the branching factor of a balanced tree while keeping the number of sinks constant. For example, a balanced tree with a binary branching factor driving 16 sinks has five levels and is equivalent to a five-section ladder circuit. If the same 16 sinks are driven by a balanced tree with a branching factor equal to 16, the tree has only two levels and is equivalent to a two-section ladder circuit. Thus, the second-order approximation more accurately describes an RLC tree with a branching

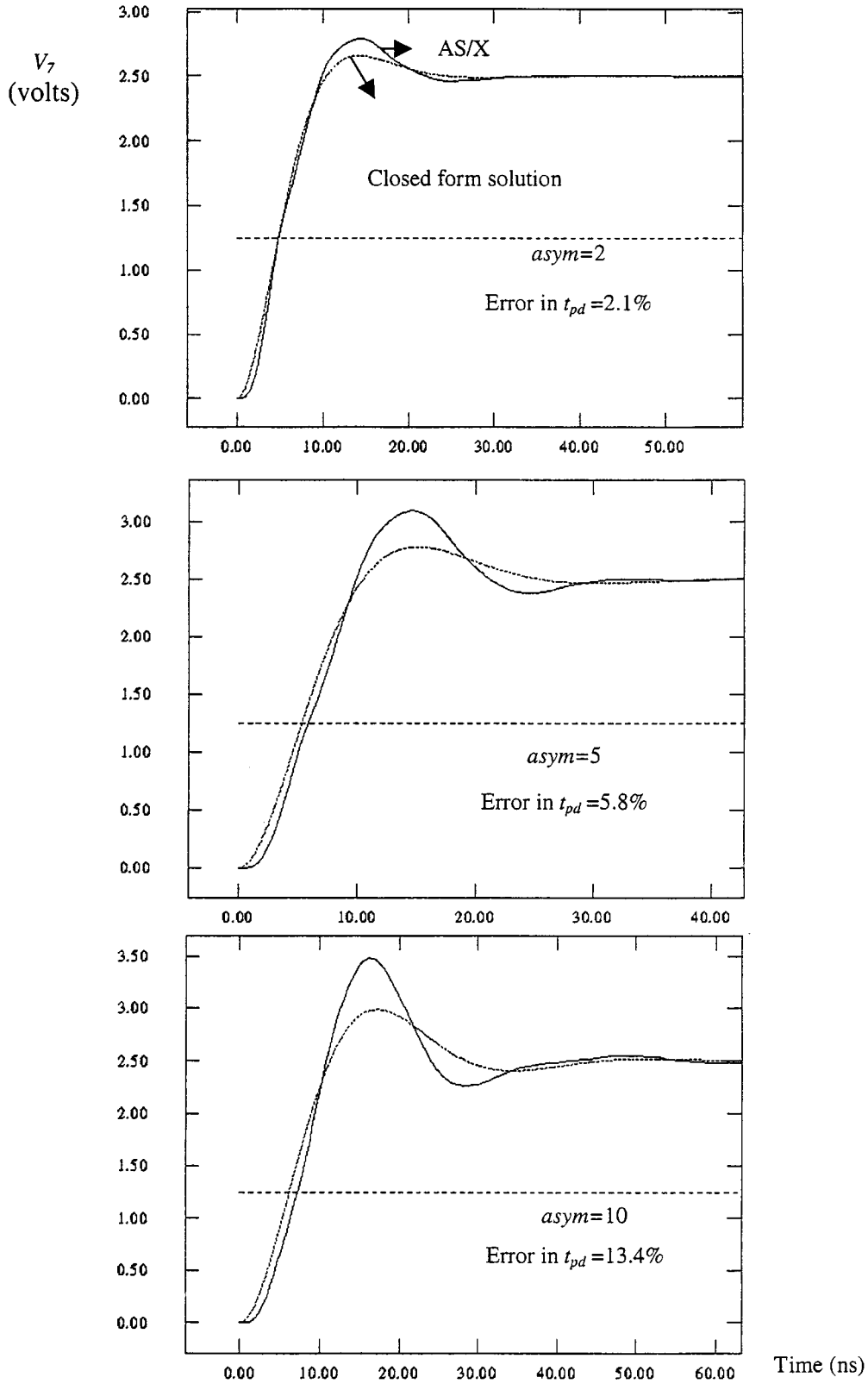

Fig. 12. AS/X simulations as compared to (31) for several asymmetric trees. Results are for node 7 for the circuit shown in Fig. 5.

factor equal to 16. AS/X simulations and the closed-form solution from (31) with a step input for the response at the sinks of both trees are shown in Fig. 13. In this example, all of the RLC sections in the binary branching tree has $R = 12.5\ \Omega, L = 5$ nH, and $C = 1$ pF. All of the RLC sections in the tree with a branching factor of 16 has $R = 25\ \Omega, L = 5$ nH, and $C = 1$ pF. Note that the second-order approximation is less accurate in the case of a tree with a binary branching factor.

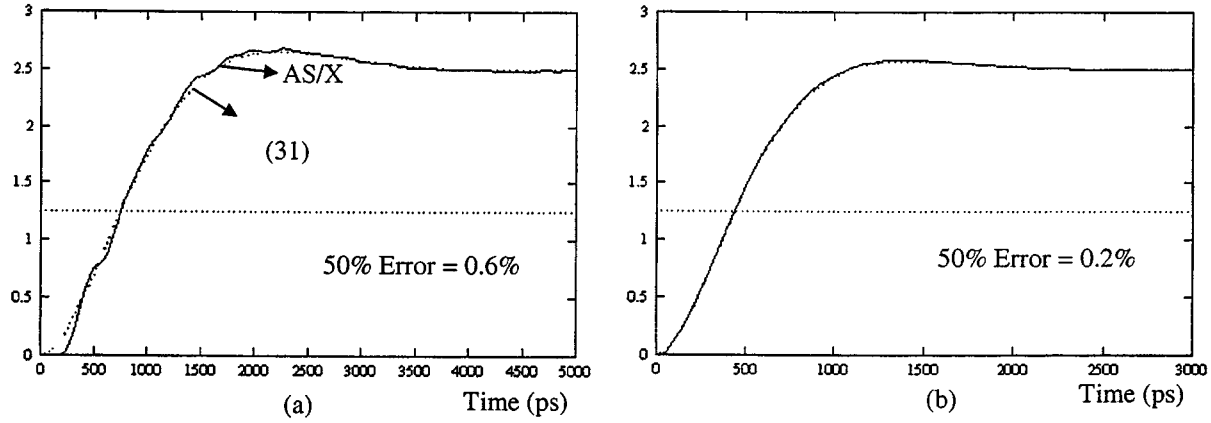

Fig. 13. AS/X simulations as compared to (31) for the response at the 16 sinks of a balanced tree. (a) The tree has a binary branching factor. (b) The tree has a branching factor of 16.

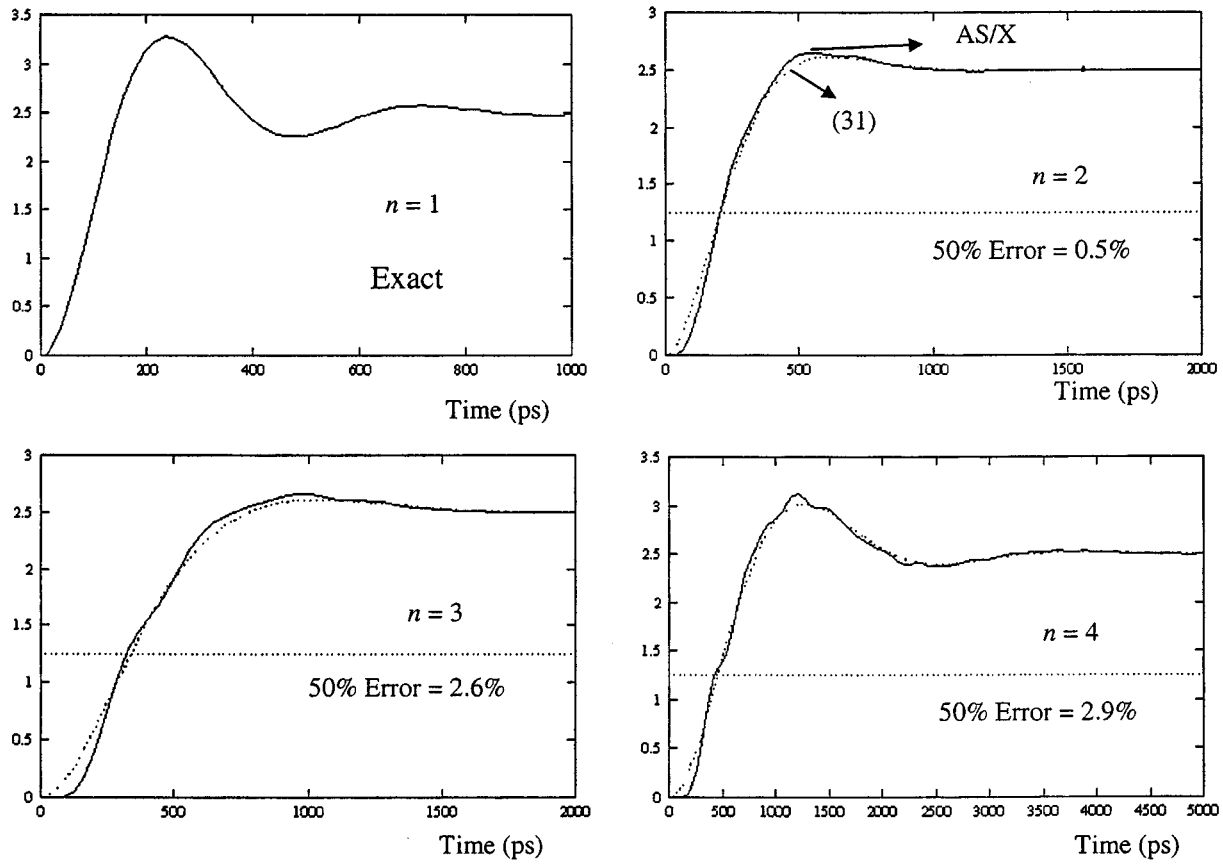

Fig. 14. AS/X simulations as compared to (31); for several balanced trees with different depths.

D. Effect of the Depth of the Tree

The depth of a tree can be characterized by the number of levels n of the tree. The accuracy of the solution decreases as the number of levels in the tree increases since the order of the transfer function at the sinks increases. The increased error due to increasing the depth of the tree can be best observed for a balanced tree since the error due to the unbalance overrides the error due to the depth in an unbalanced tree. AS/X simulations are compared to (31) in Fig. 14 for balanced trees with a different number of levels. Note that the error between AS/X and the closed-form solution increases as the number of levels of the tree increases. Note also that for a single line, the depth represents the number of sections of the line.

E. Effect of the Node Position

The error exhibited by the second-order approximation increases as the position of the node at which the response is evaluated moves from the sinks toward the source. This behavior is due to the extra finite zeros in the transfer function since there are less capacitors and inductors in the path from the input to the node at which the response is evaluated. Again, this effect is best observed for a balanced tree. AS/X simulations are compared to (31) in Fig. 15 at several positions of the five-level binary bal-

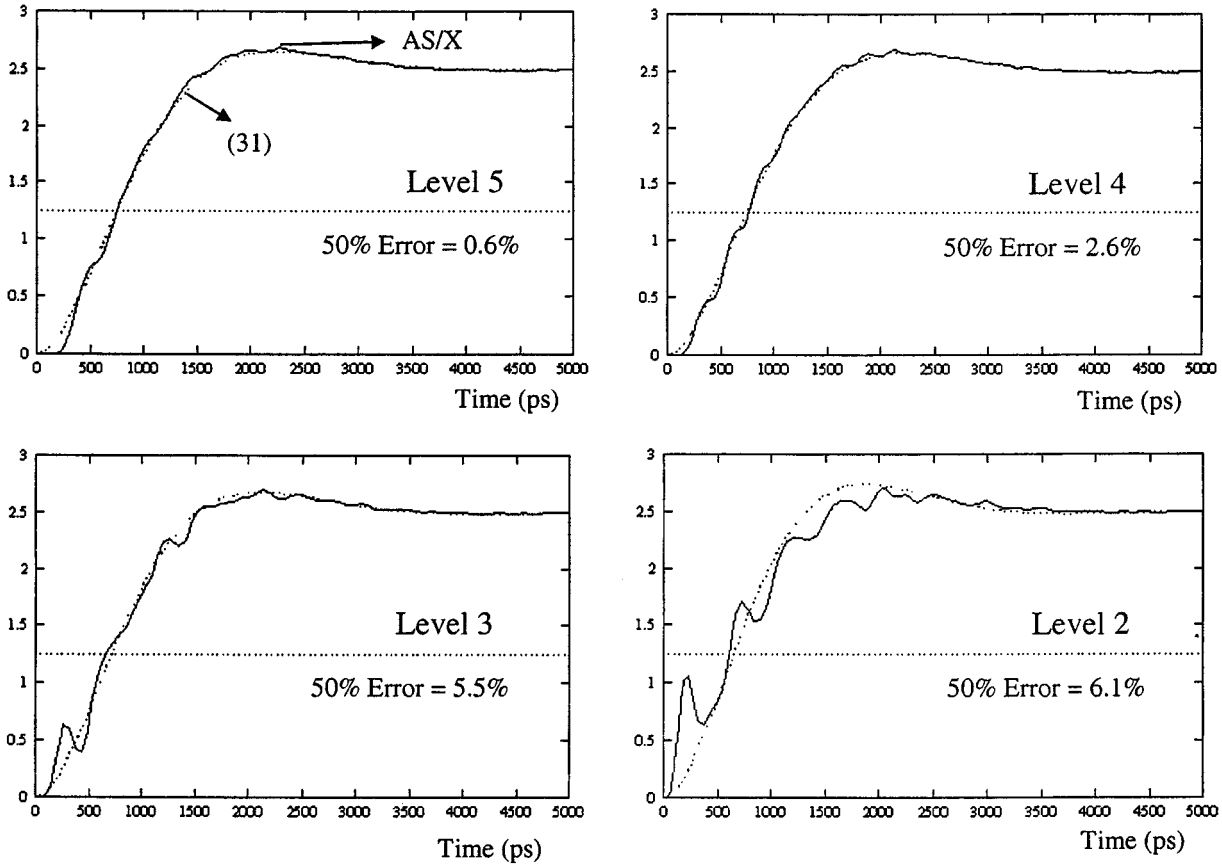

Fig. 15. AS/X simulations as compared to (31) for a binary balanced tree for nodes at different levels within the tree.

anced tree described in Section V-C. Note that the error between AS/X and the closed-form solution is least at the sinks which is typically the location of greatest interest.

F. Effect of Second-Order Oscillations

As an RLC tree becomes larger and as the number of levels increase, high-frequency oscillations are superimposed over the primary response. For example, in Fig. 16, the second-order approximation (31) of the response for a large RLC tree is illustrated. Note the overshoots. AS/X simulations are also shown in Fig. 16 and the actual signal oscillates around the second-order approximation with a higher frequency as compared to the frequency of the primary oscillations. The oscillations around the low-frequency response characterized by (31) are second-order oscillations. The second-order approximation introduced here cannot accurately model the higher frequency harmonics of the time domain response since it only has two poles. However, the second-order approximation can be used effectively to estimate the macro features of the response such as the propagation delay, the rise time, and the primary overshoots. If the fine details of the response are of interest, higher-order delay models can be used such as AWE [33]–[35] at the expense of additional processing time, numerical issues, and stability issues. Note that the responses in the simulations presented in this section also exhibit second-order oscillations. The second-order approximation successfully characterizes the dominant low-frequency response.

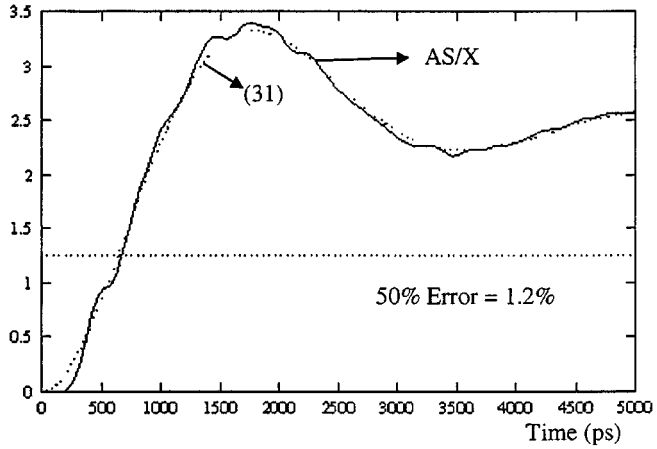

Fig. 16. AS/X simulations as compared to (31) for a large RLC tree.

VI. Conclusion

A general method to characterize the response of a linear nonmonotone system that is equivalent to the Elmore delay is presented. The generated delay expressions for an RLC tree have the same accuracy characteristics as the Elmore (Wyatt) approximation for RC trees. Simple analytical expressions of signals in an RLC tree are provided for the 50% delay, the rise time, overshoots, and settling time. These expressions consider both monotone and nonmonotone signal responses. The delay expressions are continuous and hence are useful for optimization and synthesis in VLSI-based design methodologies.

The second-order approximation introduced here is always stable and can be used with arbitrary inputs. Furthermore, the second-order approximation is computationally efficient since the number of multiplication operations required to evaluate the approximation at all of the nodes of an RLC tree is linearly proportional to the number of branches in the tree.

APPENDIX
COMPLEXITY OF THE SECOND-ORDER APPROXIMATION

Referring to (13), (29), and (30), the second-order approximate transfer function at node i is

$$g_i(s) = \frac{1}{\left[\sum_k C_k L_{ik}\right] s^2 + \left[\sum_k C_k R_{ik}\right] s + 1}. \quad (49)$$

Thus, evaluating this transfer function for all of the nodes of an RLC tree requires the calculation of the following two summations:

$$T_{RCi} = \sum_k C_k R_{ik} \quad (50)$$

$$T^2_{LCi} = \sum_k C_k L_{ik} \quad (51)$$

for all of the nodes of the RLC tree. These two summations can be rewritten as

$$T_{Rci} = \sum_k C_{Tk} R_k \quad (52)$$

$$T^2_{LCi} = \sum_k C_{Tk} L_k \quad (53)$$

where the summation index k operates over all of the RLC sections that belong to the path from the input to node i. R_k and L_K is the resistance and inductance of section k. C_{Tk} is the total load capacitance seen by R_k and L_K. For example, in Fig. 5, $T_{RC7} = R_1(C_1+C_2+\cdots+C_7)+R_6(C_3+C_6+C_7)+R_7C_7$. This form of expressing the summations is convenient since it has recursive properties [29], [48].

The summations in (52) and (53) of a tree rooted at section $w1$ are calculated in two steps. The first step is to calculate the total load capacitance seen by each section. Pseudocode that performs this task is described in Fig. 17.

The function is initially called by Cal_Cap_Loads(w_1) and recursively calculates the capacitive load at each section. $w.C$ is the capacitance of the section w. The functions, left(w) and right(w), return the left and right sections driven by w, respectively. If no left (right) section is driven by w, left(w) $= 0$ (right(w) $= 0$). If w is a leaf, left(w) $= 0$ and right(w) $= 0$. The time required to calculate the total capacitive loads is proportional to the number of RLC sections in the tree m, and requires no multiplication operations. Note that a binary branching factor is assumed without loss of generality since any general tree can be transformed into a binary tree by inserting wires with zero impedances [27], [28].

```
float Cal_Cap_Loads (section w)
{
        if(right(w)=0 and left(w)=0)    /* if w is a leaf */
                return w.C;

        if(right(w)≠0)
                C_TR=Cal_Cap_Loads(right(w));
        else
                C_TR=0;      /* No right branch is driven by w */

        if(left(w)≠0)
                C_TL=Cal_Cap_Loads(left(w));
        else
                C_TL=0;      /* No left branch is driven by w */

        w.C_T=C_TR+C_TL;

        return w.C_T;
}
```

Fig. 17. Pseudocode for calculating the total load capacitance at each section.

```
Cal_Summations(section w, float T_Rcprev, float T_LCprev)
{
        T_RC=T_Rcprev+w.R*w.C_T;
        T_LC=T_Rcprev+w.L*w.C_T;


        if(right(w)≠0)
                Cal_ Summations (right(w),T_RC,T_LC);

        if(left(w)≠0)
                Cal_ Summations (left(w),T_RC,T_LC);
}
```

Fig. 18. Pseudocode for calculating the delays at the sinks of an RLC tree.

The second step is to calculate and store the summations in (52) and (53) at the nodes of the tree. The function performing this task is described in Fig. 18. The function is initially called by Cal_Summations($w_1, 0, 0$). $w.R$ and $w.L$ are the resistance and inductance of section w, respectively. The computational time required to calculate the summations is proportional to the number of RLC sections in the tree m. The total number of multiplications required to evaluate the second-order approximation at all of the nodes of an RLC tree is $2m$. Alternatively, the number of multiplications is equal to the order of the characteristic equation describing the RLC tree since the order of an RLC tree with m RLC sections is $2m$ (each RLC section has an inductor and a capacitor).

REFERENCES

[1] J. M. Rabaey, *Digital Integrated Circuits, A Design Perspective*. Englewood Cliffs, NJ: Prentice-Hall, 1996.

[2] D. A. Priore, "Inductance on silicon for sub-micron CMOS VLSI," in *Proc. IEEE Symp. VLSI Circuits*, May 1993, pp. 17–18.

[3] D. B. Jarvis, "The effects of interconnections on high-speed logic currents," *IEEE Trans. Electron. Comput.*, vol. EC-10, pp. 476–487, Oct. 1963.

[4] Y. Eo and W. R. Eisenstadt, "High-speed VLSI interconnect modeling based on S-parameter measurement," *IEEE Trans. Comp., Hybrids, Manufac. Technol.*, vol. 16, pp. 555–562, Aug. 1993.

[5] A. Deutsch *et al.*, "High-speed signal propagation on lossy transmission lines," *IBM J. Res. Develop.*, vol. 34, no. 4, pp. 601–615, July 1990.

[6] ——, "Modeling and characterizing of long interconnections for high-performance microprocessors," *IBM J. Res. Develop.*, vol. 39, no. 5, pp. 547–667, Sept. 1995.
[7] ——, "When are transmission-line effects important for on-chip interconnections?," *IEEE Trans. Microwave Theory Tech.*, vol. 45, pp. 1836–1846, Oct. 1997.
[8] Y. I. Ismail, E. G. Friedman, and J. L. Neves, "Figures of merit to characterize the importance of on-chip inductance," in *Proc. IEEE/ACM Design Automation Conf.*, June 1998, pp. 560–565.
[9] M. P. May, A. Taflove, and J. Baron, "FD-TD modeling of digital signal propagation in 3-D circuits with passive and active loads," *IEEE Trans. Microwave Theory Tech.*, vol. 42, pp. 1514–1523, Aug. 1994.
[10] T. Sakurai, "Approximation of wiring delay in MOSFET LSI," *IEEE J. Solid-State Circuits*, vol. SC-18, pp. 418–426, Aug. 1983.
[11] G. Y. Yacoub, H. Pham, and E. G. Friedman, "A system for critical path analysis based on back annotation and distributed interconnect impedance models," *Microelectron. J.*, vol. 18, no. 3, pp. 21–30, June 1988.
[12] J. Torres, "Advanced copper interconnections for silicon CMOS technologies," *Appl. Surface Sci.*, vol. 91, no. 1, pp. 112–123, Oct. 1995.
[13] C. F. Webb *et al.*, "A 400 MHz S/390 microprocessor," in *Proc. IEEE Int. Solid-State Circuits Conf.*, Feb. 1997, pp. 448–449.
[14] P. J. Restle and A. Deutsch, "Designing the best clock distribution network," in *Proc. IEEE VLSI Circuit Symp.*, June 1998, pp. 2–5.
[15] W. C. Elmore, "The transient response of damped linear networks," *J. Appl. Phys.*, vol. 19, pp. 55–63, Jan. 1948.
[16] J. L. Wyatt, *Circuit Analysis, Simulation and Design*. North-Holland, The Netherlands: Elsevier Science, 1987.
[17] J. Cong, L. He, C.-K. Koh, and P. Madden, "Performance optimization of VLSI interconnect," *Integration, VLSI J.*, vol. 21, pp. 1–94, Nov. 1996.
[18] J. Cong and K. S. Leung, "Optimal wire sizing under the distributed Elmore delay model," in *Proc. IEEE/ACM Int. Conf. Computer-Aided Design*, Nov. 1993, pp. 634–639.
[19] J. Cong and C.-K. Koh, "Simultaneous driver and wire sizing for performance and power optimization," *IEEE Trans. Very Large Scale Integration (VLSI) Syst.*, vol. 2, pp. 408–423, Dec. 1994.
[20] K. D. Boese, A. B. Kahng, and G. Robins, "High-performance routing trees with identified critical sinks," in *Proc. IEEE/ACM Design Automation Conf.*, June 1993, pp. 182–187.
[21] K. D. Boese, A. B. Kahng, B. A. McCoy, and G. Robins, "Rectilinear Steiner trees with minimum Elmore delay," in *Proc. IEEE/ACM Design Automation Conf.*, June 1994, pp. 381–386.
[22] S. S. Sapatnekar, "RC interconnect optimization under the Elmore delay model," in *Proc. IEEE/ACM Design Automation Conf.*, June 1994, pp. 387–391.
[23] J. Cong and L. He, "Optimal wire sizing for interconnects with multiple sources," in *Proc. IEEE/ACM Design Automation Conf.*, Nov. 1995, pp. 586–574.
[24] L. W. Nagel, "SPICE2: A computer program to simulate semiconductor circuits," Univ. California, Berkeley, CA, Tech. Rep.t ERL-M520, May 1975.
[25] K. D. Boese, A. B. Kahng, B. A. McCoy, and G. Robins, "Fidelity and near-optimality of Elmore-based routing constructions," in *Proc. IEEE Int. Conf. Computer Design*, Oct. 1993, pp. 81–84.
[26] J. Cong, A. B. Kahng, C.-K. Koh, and C.-W. A. Tsao, "Bounded-slew clock and Steiner routing under Elmore delay," in *Proc. IEEE Int. Conf. Computer-Aided Design*, Jan. 1995, pp. 66–71.
[27] L. P. P. P. van Ginneken, "Buffer placement in distributed RC-tree networks for minimal Elmore delay," in *Proc. IEEE Int. Symp. Circuits and Systems*, May 1990, pp. 865–868.
[28] C. J. Alpert, "Wire segmenting for improved buffer insertion," in *Proc. IEEE/ACM Design Automation Conf.*, 1997, pp. 588–593.
[29] J. Rubinstein and P. Penfield, Jr., "Signal delay in RC tree networks," in *Proc. IEEE/ACM Design Automation Conf.*, 1983, pp. 202–211.
[30] A. B. Kahng and S. Muddu, "An analytical delay model for RLC interconnects," *IEEE Trans. Computer-Aided Design*, vol. 16, pp. 1507–1514, Dec. 1997.
[31] L. T. Pillage and R. A. Rohrer, "Delay evaluation with lumped linear RLC interconnect circuit models," in *Proc. Caltech Conf. VLSI*, May 1989, pp. 143–158.
[32] M. A. Horowitz, "Timing models for CMOS circuits," Ph.D. dissertation, Stanford Univ., Stanford, CA, Jan. 1984.
[33] L. T. Pillage, R. A. Rohrer, and C. Visweswariah, *Electronic Circuit and System Simulation Methods*. New York: McGraw Hill, 1994.
[34] L. T. Pillage and R. A. Rohrer, "Asymptotic waveform evaluation for timing analysis," *IEEE Trans. Computer-Aided Design*, vol. 9, pp. 352–366, Apr. 1990.
[35] C. L. Ratzlaff, N. Gopal, and L. T. Pillage, "RICE: Rapid interconnect circuit evaluator," in *Proc. IEEE/ACM Design Automation Conf.*, June 1991, pp. 555–560.
[36] T. K. Tang and M. S. Nakhla, "Analysis of high-speed VLSI interconnects using the asymptotic waveform evaluation techniques," *IEEE Trans. Computer-Aided Design*, vol. 11, pp. 341–352, Mar. 1992.
[37] L. T. Pillage, "Coping with RC(L) interconnect design headaches," in *Proc. IEEE/ACM Int. Conf. Computer-Aided Design*, Sept. 1995, pp. 246–253.
[38] P. Feldmann and R. W. Freund, "Efficient linear circuit analysis by Pade approximation via the Lancozos process," *IEEE Trans. Computer-Aided Design*, vol. 14, pp. 639–649, May 1995.
[39] ——, "Reduced-order modeling of large linear subcircuits via block Lanczos algorithm," in *Proc. IEEE/ACM Design Automation Conf.*, June 1995, pp. 474–479.
[40] M. Silveira, M. Kamon, and J. White, "Efficient reduced-order modeling of frequency-dependent coupling inductances associated with 3-D interconnect structures," in *Proc. IEEE/ACM Design Automation Conf.*, June 1995, pp. 376–380.
[41] D. L. Boley, "Krylov space methods on state-space control models," *J. Circuits, Syst., Signal Processing*, vol. 13, no. 6, pp. 733–758, May 1994.
[42] A. Odabasioglu, M. Celik, and L. T. Pillage, "PRIMA: Passive reduced-order interconnect macromodeling algorithm," *IEEE Trans. Computer-Aided Design*, vol. 17, pp. 645–654, Aug. 1998.
[43] ——, "PRIMA: Passive reduced-order interconnect macromodeling algorithm," in *Proc. IEEE/ACM Int. Conf. Computer-Aided Design*, Nov. 1997, pp. 58–65.
[44] P. Feldman and R. W. Freund, "Reduced-order modeling of large passive linear circuits by means of the SyPVL algorithm," in *Proc. IEEE/ACM Int. Conf. Computer-Aided Design*, Nov. 1996, pp. 280–287.
[45] A. B. Kahng, K. Masuko, and S. Muddu, "Analytical delay models for VLSI interconnects under ramp input," in *Proc. IEEE Int. Conf. Computer-Aided Design*, Nov. 1996, pp. 30–36.
[46] *AS/X User's Guide*. New York, NY: IBM Corp., 1996.
[47] B. C. Kuo, *Automatic Control Systems, A Design Perspective*. New Delhi, India: Prentice-Hall, India, 1989.
[48] C. L. Ratzlaff, "A Fast Algorithm for Computing the Time Moments of RLC Circuits," masters thesis, Univ. Texas at Austin, Austin, TX, May 1991.
[49] Y. I. Ismail, E. G. Friedman, and J. L. Neves, "Equivalent Elmore Delay for RLC Trees," in *Proc. IEEE/ACM Design Automation Conf.*, June 1999, pp. 715–720.

Yehea I. Ismail received the B.S. degree in electronics and communications engineering from Cairo University, Cairo, Egypt in 1993 (distinction with honors). He received the first M.S degree in electronics from Cairo University (distinction), in 1996 and the second M.S in electrical engineering from the University of Rochester, Rochester, NY, in 1998. He is currently working toward the Ph.D. degree in the area of high-performance VLSI integrated circuit design.

He was with IBM Cairo Scientific Center (CSC) from 1993 to 1996 and worked with IBM Microelectronics at East Fishkill, NY, for the summers of 1997, 1998, and 1999. His primary research interests include interconnect, noise, and related circuit-level issues in high-performance VLSI circuits.

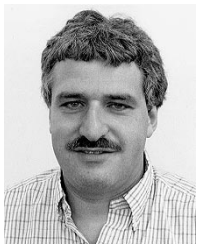

Eby G. Friedman (S'78–M'79–SM'90–F'00) received the B.S. degree from Lafayette College, Easton, PA, in 1979, and the M.S. and Ph.D. degrees from the University of California, Irvine, in 1981 and 1989, respectively, all in electrical engineering.

From 1979 to 1991, he was with Hughes Aircraft Company, rising to the position of Manager of the Signal Processing Design and Test Department, responsible for the design and test of high-performance digital and analog integrated circuits. He has been with the Department of Electrical and Computer Engineering at the University of Rochester since 1991, where he is a Professor, the Director of the High Performance VLSI/IC Design and Analysis Laboratory, and the Director of the Center for Electronic Imaging Systems. His current research and teaching interests are in high-performance synchronous digital and mixed-signal microelectronic design and analysis with application to high-speed portable processors and low-power wireless communications. He is the author of more than 125 papers and book chapters and the editor of three books in the fields of high-speed and low-power CMOS design techniques, high-speed interconnect, and the theory and application of synchronous clock distribution networks. He is a Regional Editor of the *Journal of Circuits, Systems, and Computers* and, a member of the editorial board of *Analog Integrated Circuits and Signal Processing*, and a member of the CAS BoG. Dr. Friedman is a member of the Editorial Board of IEEE TRANSACTIONS ON CIRCUITS AND SYSTEMS II: ANALOG AND DIGITAL SIGNAL PROCESSING, and Chair of the IEEE TRANSACTIONS ON VLSI SYSTEMS steering committee. He is a member of the technical program committee of a number of conferences.

He previously was a Member of the Editorial Board of the IEEE TRANSACTIONS ON CIRCUITS AND SYSTEMS II: ANALOG AND DIGITAL SIGNAL PROCESSING. He was Chair of the VLSI Systems and Applications CAS Technical Committee, Chair of the VLSI track for ISCAS '96 and '97, and Editor of several special issues in a variety of journals, Chair of the Electron Devices Chapter of the IEEE Rochester Section, Technical Co-Chair of the 1997 IEEE International Workshop on Clock Distribution Networks. He was a recipient of the Howard Hughes Masters and Doctoral Fellowships, an IBM University Research Award, an Outstanding IEEE Chapter Chairman Award, and a University of Rochester College of Engineering Teaching Excellence Award.

José L. Neves (S'89–M'96) received the B.S. degree in electrical engineering (1986) and an M.S. degree in computer science (1989) from the Federal University of Minas Gerais (UFMG), Brazil. He received the M.S. and Ph.D. degrees in electrical engineering from the University of Rochester, Rochester, NY in 1991 and 1995, respectively.

He has been with EDA/IBM Server Group as an Advisory Engineer/Scientist responsible for the development and implementation of CAD design system software in the areas of clock distribution design, high-performance clock routing, timing optimization, and optimization of power distribution. Lately, he has been involved in the design and implementation of an integrated system targeting signal integrity, including capacitive and inductive coupling effects on timing and noise, power-supply analysis and design, and noise correction capabilities.

His research interests include high-performance VLSI/IC design and analysis, algorithmic optimization techniques for timing, noise, and power distribution, and design and synthesis of high-performance clock distribution networks. He is also active on the specification of design methodologies/CAD systems targeting high-performance, high-volume integrated circuit designs.